URANS MODELLING FOR MIXED CONVECTION THERMAL TRANSIENTS IN A U-BEND

Minto Kavyan[1*], Hector Iacovides[1], Alex Skillen[1], Andrea Cioncolini[1]

[1]Thermo-Fluids Group, Department of Mechanical, Aerospace and Civil Engineering, University of Manchester, Manchester M13 9PL, United Kingdom

ABSTRACT

The focus of this study is the transient mixed convection flow that develops in a 180° turn of circular cross-section, with vertical downward inlet a horizontal middle and a vertical upward exit section, as a result of a linear increase in the inlet temperature. The working fluid is water, Pr = 6, at a Reynolds number of 10,000. The thermal development is further complicated by heat conduction along the pipe wall, requiring conjugate heat transfer analysis. The objective is to assess the effectiveness of unsteady RANS models. At this stage the flow is treated as 2-dimensional. Turbulent stresses are modelled using eddy-viscosity based two-equation models, either a high (k–ε), or low (Launder–Sharma k–ε and k-ω SST) Reynolds-number versions. Computations have been produced both with and without accounting for the direct effects of buoyancy on the generation rate of turbulence, the latter being the 'standard' practice in the OpenFoam CFD software employed in this study.

The resulting predictions are compared against the available experimental data by Viollet [1]. The 2-D URANS computations, the wall temperature variation are surprisingly close to the corresponding measurements. This is because the flow and thermal developments are dominated by thermal stratification and the curvature-induced stream-wise pressure gradients. To reliably compute these complex phenomena the direct effects of buoyancy on turbulence generation needs to be included and the use of log-law-based wall functions needs to be avoided. The Launder-Sharma predictions are found to be the most reliable.

1. INTRODUCTION

U-bend shaped pipes are relevant to the secondary circuit (outlet of Steam-Generator) of a Fast Breeder Reactor. Analysing the dynamics of flow, as a thermal transient passes through the whole domain of the passage considered here, is relevant to nuclear thermal hydraulic applications. A key feature at low flow rates, is the strong thermal stratification along the horizontal section of the bend (see Fig. 1), which results in large temperature differences. An experimental study conducted by Viollet [1] looked at the thermal transients (linear ramp over a short period at the inlet), both hot and cold, in a U-bend with low Reynolds and Froude numbers, and thermal stratification was observed. This stratification can cause significant changes to the flow, like steep temperature gradients and large recirculation regions.

As experimental investigations are expensive and high-fidelity CFD (Computational Fluid Dynamics) simulations like LES (Large Eddy Simulations) and DNS (Direct Numerical Simulation) demand prohibitively high computational resources, the potential of RANS (Reynolds-averaged Navier-Stokes simulations) turbulence models is explored here. The objective of this study is to identify the URANS models which can reliably reproduce the physical phenomena discussed above; this is achieved by evaluating the performances of these models against the experimental data of Viollet [1].

2. MODELLING

In the RANS approach to the simulation of turbulent flows, the transport equations for the mean momentum and enthalpy contain additional terms, the turbulent stresses and heat fluxes respectively. The turbulent stresses are modelled using eddy-viscosity-based two-equation models, either a high low-

*Corresponding Author: minto.kavyan@postgrad.manchester.ac.uk

Reynolds-number version, employing wall functions (based on the log-law) or low-Reynolds-number ones, as detailed in Table 1. The turbulent heat fluxes are modelled using the eddy-diffusivity approach. Computations are performed with and without considering the direct effects of buoyancy on the turbulence generation rate. The different versions of the model tested are detailed in Table 2.

Two different meshes, using structured hexahedral control volumes, are used, depending on the near-wall approaches considered in this study. The y^+ values of near-wall nodes are greater than 30 and around 1 for the wall function and the low-Re approaches respectively. After testing for grid independence, 35880 cells and 67256 cells have been adopted for these two approaches respectively. To account for conjugate heat transfer, meshing is extended to the solid wall regions.

Table 1: Turbulence models and wall treatments tested within this study.

Reynolds stresses	Near-Wall Strategy	Name	Reference
Low-Re k– ε (Launder Sharma)	Fine near-wall grid	LRN	Launder & Sharma [2]
High-Re k– ε	Standard wall function	HRN	Launder and Spalding [3]
k-ω SST	Fine near-wall grid	SST	Menter [4]

Table 2: Models tested, and the physics included.

Turbulence model versions	Physics included
Version 1	Model without buoyancy generation
Version 2	Model with buoyancy generation included.
Version 3	Model with buoyancy generation and conjugate heat transfer included.
Version 4	Model with buoyancy generation, conjugate heat transfer and variable fluid property (variable density) included.

3. CASE SET-UP

The experimental setup used by Viollet [1] is considered with an extended downstream vertical section, as shown schematically in Fig. 1. The configuration tested is a U-bend shaped pipe with smooth walls, a downward slope of 1% at the near-horizontal section and a circular cross-section throughout, having an inner diameter (D) of 0.25 m. Here, we approximate the flow as a 2D curved channel in our preliminary analysis. Transient simulations for hot thermal transient propagating through the channel are performed by selecting the hot shock case with a Reynolds number (the flow Re is based on bulk velocity) of 10000 considered by Viollet [1]. The working fluid for the simulation is taken as water, at an initial inlet temperature of 299 K, Prandtl number (Pr) of 6 and a Richardson number ($\mathrm{Ri} = g\beta(T_1 - T_0)D / U^2$, where g, β, T_0, and U are acceleration due to gravity, thermal expansion coefficient, reference temperature and bulk velocity respectively) of 14.73. At the inlet, the temperature linearly increases to 326 K over the transient period and then remains constant. Table 3 lists the boundary conditions applied. Simulations have been performed in OpenFoam v1912 using the finite volume method. This includes the PIMPLE algorithm for the pressure field, and the QUICK convective discretization scheme.

Table 3: Boundary conditions used in this study (CHT represents Conjugate Heat Transfer).

Boundary conditions	u (m/s)	p (Pa)	T (K)	k (m^2/s^2)	ε (m^2/s^3)	ω (m^2/s^3)
Inlet	0.0349	Zero grad.	Variable value	1.8291 e-05	3.45 e-06	2.0952
Fluid-solid interface	No-slip	Zero grad.	CHT	Zero / WF	Zero / WF	WF
Outlet	Zero grad.	Zero	Zero grad.	Zero grad.	Zero grad.	Zero grad.
Outer wall surface	-	-	Zero grad.	-	-	-

4. RESULTS

4.1 Flow Development

The main characteristics of the flow development are highlighted in the contour and streamline plots of Figure 3. After the first turn, along the horizontal section, the hotter, lighter, fluid is pushed towards the upper half of the channel and accelerates, while the lower half of the channel is occupied by cooler and slow recirculating fluid. This is a result of the combined effect of the first turn, as the contact surface between cold and hot fluid approaches the first bend, the fluid along the inner, upper, surface is accelerated thus transferring the hotter fluid along this side, whilst the buoyancy force, which maintains this thermal stratification along the horizontal section. Buoyancy forces preserve this stratification in the near-horizontal section and thus a stable stratification is observed. The second turn further accelerates the fluid along the inner (upper) side, causing a large separation bubble along the outer side, at the turn exit. As the fluid moves further downstream along the vertical section, an oscillatory behaviour can be seen, in which the faster fluid switches to the outer side and flow separation appears along what was the inner side of the channel. The turbulent viscosity contour plot indicates that a) along the horizontal section the stable thermal stratification suppresses turbulence along the lower half, and b) in the vertical section downstream of the second turn, where the flow is more complex, turbulence is substantially stronger.

4.2 Influence of Buoyancy Generation Term, Conjugate Heat Transfer and Variable Fluid Properties

For an assessment of the effects of buoyancy generation of turbulence, conjugate heat transfer and variable fluid properties, on the flow and thermal development, attention is first focused on Figure 4. It compares temperature profiles along the two channel walls, predicted by the different versions of the Launder–Sharma (L-S) k–ε model listed in Table 2, with the corresponding measurements from [1]. The model versions which include buoyancy generation can capture the effects of thermal stratification along the horizontal section (highlighted in Figure 3 and later in Figure 5). They return lower temperatures along the lower wall, which are in accord with the measurements.

Figure 5 presents profiles of temperature, velocity and turbulent kinetic energy at 3 diameters downstream of the first bend, also using the four versions of the L-S k–ε model examined in Figure 4, at a time of 150 seconds from the start of the transient. The temperature profile comparisons show that the turbulence model without buoyancy generation over-estimates the lower wall temperature in the horizontal section and thus provide a more quantitative demonstration regarding the inability of such models to reproduce the lower wall temperature. As expected, up to the second bend, for all stages of the transient, similar results are produced by versions 2-4 of the L-S model, all of which include the buoyancy generation term. The model versions which include buoyancy generation capture the characteristic feature, recirculation region along the lower wall of the horizontal section, up to the last stage of the transient, where thermal stratification is evident. Since without buoyancy generation, the L-S model cannot predict the thermal stratification, which drives the buoyancy forces which generate such recirculation regions, it is no surprise that it fails to capture this phenomenon. The recirculation region near the lower wall receives limited heat transfer due to the existence of thermal transient for a long time.

The effects of the buoyancy generation term is again highly noticeable in the comparisons of the turbulent kinetic energy profiles of Figure 5. They show that the buoyancy generation term severely suppresses turbulence levels over the lower half of the horizontal section. As indicated by the corresponding temperature profiles, there is a strong and stable thermal stratification, over this region (temperature increases in the vertical direction) which makes the buoyancy generation term negative. The lower turbulence levels over the lower half of the horizontal section result in the prediction of flow separation observed in the velocity plots. The small differences in the profiles returned by the model

versions 2-4, suggest that conjugate heat transfer and variable fluid properties have only a minor impact on the transient mixed convection flow considered here.

Conjugate heat transfer does not have much effect on temperature predictions, because the wall is made of plexiglass (a low thermal conductivity material, 0.17 W/m K). Deviations in wall temperature predictions are noticed between versions 2-4 of the model, from the second bend, for all stages of the transient. This is a region of unstable thermal stratification, where substantial mixing occurs due to large-scale turbulent structures. The temporal evolution of temperature in this region (figure not included due to space restrictions) shows that the temperature variation rate reduces with time due to mixing. If the pipe wall was made of high thermal conductivity material, we would expect to see noticeable differences between the versions of the model with and without conjugate heat transfer analysis. In the corresponding three-dimensional case, such as the one of the experimental study [1], there is also secondary motion generated by the turns, which, as recently reported [5], is reversed. The fact that the wall temperature profile comparisons show close agreement between the current 2-D predictions and the 3-D measurements over the horizontal section and the second turn, suggests that over these regions the turn streamwise pressure gradients and thermal stratification, which are primarily 2-dimensional, are the dominant influences.

4.3 Comparison of Different Turbulence Models

Figure 6 compares the wall temperature variations at the three different stages of the transient, predicted by the three turbulence models, listed in Table 1, all of which include the buoyancy generation term, variable property effects and conjugate heat transfer analysis. Upstream of the first bend, at all the three stages of the transient, temperature predictions along both the walls by all the turbulence models under consideration are quantitatively in good agreement with the experimental data. In this region of the channel flow, good predictions are expected, because there are no recirculation regions (see Figure 3), which is a challenge for any turbulence model.

Between the bends, at all the three stages of the transient, upper wall predictions are again in good agreement with the experimental data, but for the lower wall, a significant difference in predictions is evident between two low-Re and the high-Re model, with the latter over-estimating the lower wall temperature. High-Re models use wall functions based on the ‘log-law’, an assumption that is not appropriate in mixed convection flows. Near the second bend, small differences start to emerge between Launder–Sharma k–ε and k-ω SST predictions.

After the second bend, especially for the first two stages of the transient, the high-Re k-ε and the k-ω SST predict an oscillatory temperature variation along both walls which is in contrast to the variations returned by the low-Re L-S model. As indicated by the streamlines of Figure 3, downstream of the second bend the mean flow also exhibits oscillatory behaviour, with the faster fluid switching between the two sides of the channel. The wall temperature comparisons suggest that the high-Re k-ε and the k-ω SST return stronger oscillations in mean flow than the Low-Re L-S. This feature is consistent with the higher levels of turbulent viscosity returned by the low-Re L-S model in the downstream vertical section, shown in the contour comparisons of Figure 7. Due to the limited experimental measurements over this region, it is not possible to definitively establish which model prediction of the wall temperature variation after the second bend is closest to the experimental data, the distributions returned by the low-Re L-S model appear to be the ones most likely to represent the real behaviour. More detailed experimental data, or use of higher fidelity LES or DNS methods are needed for a more definitive assessment of the downstream region predictions.

.

5. CONCLUSIONS

The comparisons between the 2-dimensional Unsteady RANS simulations of transient conjugate mixed convection in a U-turn, a case similar to what is found in nuclear applications, have led to the following conclusions.

- For the region from the inlet to the second turn, where most experimental data are available. the 2-D URANS predictions of the wall temperatures are in close accord with the measured variation. This suggests that for this part of the passage, the flow development is dominated by the largely 2-dimetional turn generated streamwise pressure gradients and buoyancy generated thermal stratification.
- The use of the "log-law-based" wall functions results in predictive deficiencies, necessitating the use of low-Reynolds number turbulence models.
- Among the model tested, the Launder-Sharma k-ε models was the most effective.
- The inclusion of direct turbulence generation due to buoyancy, is essential in order to account for the effects of thermal stratification and result in reliable flow and thermal computations.
- Inclusion of the conjugate heat transfer analysis has only minor effects on the simulations, most likely because of the low thermal conductivity of the pipe walls.

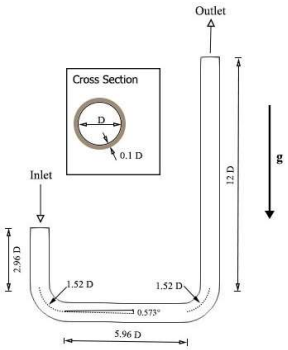

Figure 1: Schematic of the scale-model used by [1].

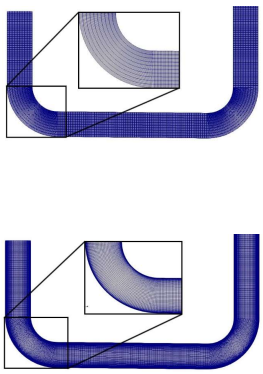

Figure 2: The mesh for the model (top - High-Re, bottom - Low-Re). Insert shows details in the first bend.

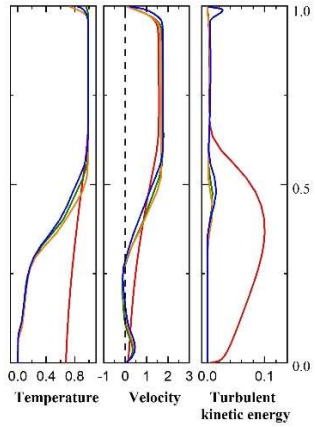

Figure 5: Profiles of normalised temperature, velocity (as in Figure 3) and turbulent kinetic energy (normalised U_0^2) at 3 diameters downstream of the first bend, at t=150s. L-S *k-ε*. Red, green, orange and blue lines indicate versions 1 - 4 (Table 2).

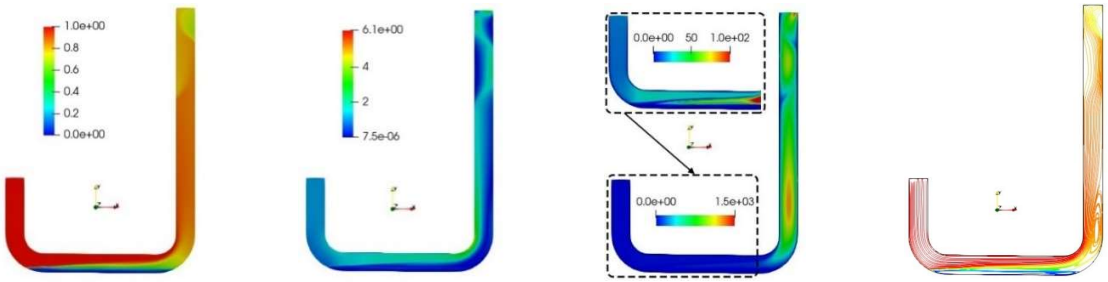

Figure 3: Flow and thermal fields at time of 200 s predicted by the L-S *k-ε*. First from left, contours of normalized velocity, U/U_B. Second left, normalized temperature $(T-T_0)/\Delta T$ (T_0 initial temperature, ΔT temperature difference between end and start of ramp). Third left, turbulent viscosity normalised by molecular viscosity. Fourth left, streamlines coloured by temperature.

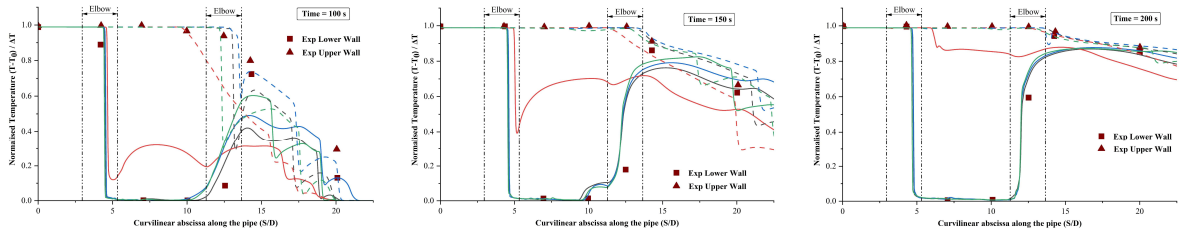

Figure 4: Comparisons of wall temperature profiles along upper (dotted line) and lower walls (solid line), at different times, predicted with the Launder–Sharma k–ε model and measured in [1]. Red, black, blue and green lines indicate versions 1-4 of the L-S model (see Table 2).

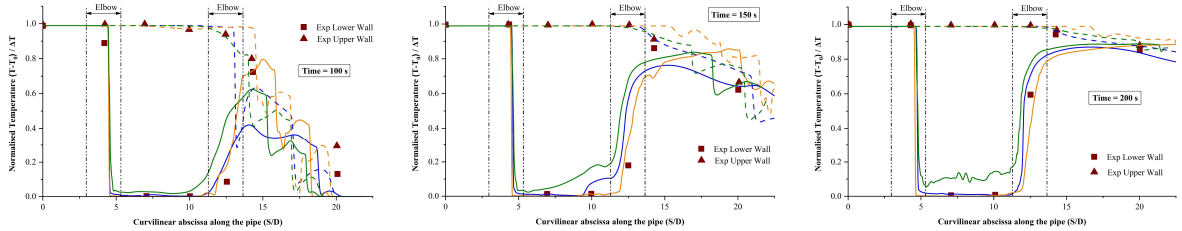

Figure 6: Comparisons of the wall temperature along upper (dotted line) and lower walls (solid line), from the Launder–Sharma k–ε (blue line), k-ω SST (orange line) and high Reynolds-number k–ε (green line) and the experimental data [1].

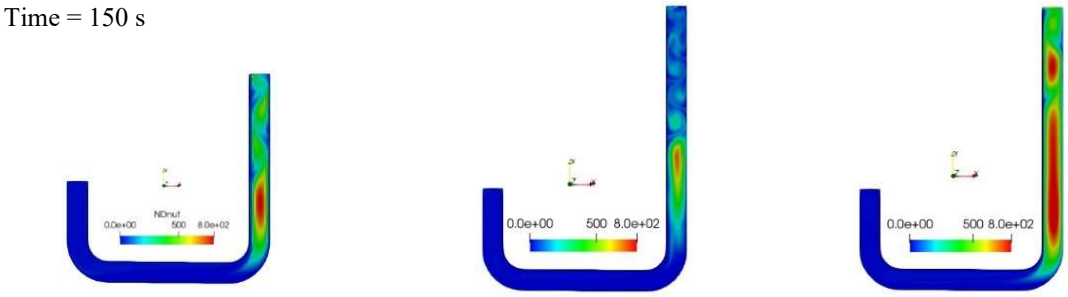

Figure 7: Predicted contours of turbulent viscosity (normalised by molecular viscosity), by different turbulence models (first, second and third figure of the row represent high Reynolds-number k–ε, k-ω SST and Launder–Sharma k–ε models respectively), version 4 (see Table 2), at the time of the transient.

REFERENCES

[1] P. L. Viollet, “Observation and numerical modelling of density currents resulting from thermal transients in a non rectilinear pipe,” *J. Hydraul. Res.*, vol. 25, no. 2, pp. 235–261, 1987.

[2] B. E. Launder and B. . Sharma, “application of the energy-dissipation model of turbulence to the calculation of flow near a spinning disc,” *Lett. heat mass Transf.*, vol. 1, pp. 131–138, 1974.

[3] B. E. Launder and D. B. Spalding, “the numerical computation of turbulent flows,” *Comput. Methods Appl. Mech. Eng.*, vol. 3, no. 2, pp. 269–289, 1974.

[4] F. R. Menter, “Two-Equation Eddy-Viscosity Turbulence Models for Engineering Applications,” *AIAA J.*, vol. 32, no. 8, 1994.

[5] A. Skillen, M. J. Zimoń, R. Sawko, R. Tunstall, C. Moulinec, and D. R Emerson, “Thermal transients in a U-bend,” *Int. J. Heat Mass Transf.*, vol. 148, pp. 1–10, 2020.